Published in final edited form as:
Surv Ophthalmol. 2014 ; 59(4): 458–467. doi:10.1016/j.survophthal.2013.04.007.

Imaging of the Optic Nerve and Retinal Nerve Fiber Layer: an Essential Part of Glaucoma Diagnosis and Monitoring

Jacek Kotowski, MD[1], **Gadi Wollstein, MD**[1], **Hiroshi Ishikawa, MD**[1], and **Joel S Schuman, MD**[1,2]

[1]Department of Ophthalmology, UPMC Eye Center, Eye and Ear Institute, Ophthalmology and Visual Science Research Center, University of Pittsburgh School of Medicine, Pittsburgh, PA

[2]Department of Bioengineering, Swanson School of Engineering, University of Pittsburgh

Glaucomatous damage specifically affects retinal ganglion cells (RGCs) and their axons and leads to progressive thinning of the retinal nerve fiber layer (RNFL) accompanied by structural changes within the optic nerve head (ONH). These changes typically appear as diffuse or focal enlargement of the optic cup corresponding to neuroretinal rim loss, displacement, barring and variation in caliber of the retinal vessels, optic disc hemorrhages, RNFL defects, and peripapillary atrophy. The detection of early glaucomatous optic nerve damage during a clinical examination is often challenging, even for experienced clinicians, because of a wide range of normal ONH appearances. Similarly, the interpretation of optic disc stereo-photographs, traditionally used to document the appearance of the ONH over time and to provide evidence of progression, is highly subjective, whereas poor quality images and differences in focus, exposure, magnification, and camera angle may often result in a false impression of progression.

The progressive loss of RGCs can lead to visual field (VF) defects. VF assessment routinely performed with standard automated perimetry (SAP) is subjective and prone to high short- and long-term inter-test variability. Because this variability can confound the assessment of VF changes over time, it is desirable to confirm these changes with objective test methods. Additionally, in many cases the loss of RGCs and resulting thinning of the RNFL and damage to the ONH have been shown to precede the onset of a glaucomatous VF defect.[22; 48; 49; 57] Because glaucomatous damage is irreversible, early detection of structural changes is imperative for timely diagnosis of glaucoma and monitoring of glaucomatous progression.

Corresponding Author: Gadi Wollstein, MD, UPMC Eye Center, 203 Lothrop Street, Pittsburgh, PA 15213; wollsteing@upmc.edu.

Conflict of Interest Disclosures: Dr. Schuman receives royalties for intellectual property licensed by Massachusetts Institute of Technology and Massachusetts Eye and Ear Infirmary to Carl Zeiss Meditec.

Considerable improvements in ocular posterior segment imaging have been made in recent years. Imaging techniques such as optical coherence tomography (OCT), scanning laser polarimetry (SLP) and confocal scanning laser ophthalmoscopy (CSLO) rely on different properties of light to provide objective structural assessment of the RNFL, ONH and macula, thus assisting clinicians in the diagnosis of glaucoma and monitoring of its progression.

ONH and RNFL Imaging For Glaucoma Diagnosis

Optical Coherence Tomography

Based on the principle of low coherence interferometry, OCT provides cross-sectional visualization of ocular structures.[26; 52; 53] Low-coherence light is aimed at a beam splitter, which splits the light and directs it to the retina and a reference mirror. The light reflected from the mirror then recombines with the light reflected from the retina creating an interference pattern caused by the altered magnitude and time delay of light as it encounters different optical reflectance across the depth of the tissue. Segmentation algorithms can be applied to the cross-sectional images to obtain retinal and RNFL thickness and ONH structural information. Stratus OCT (Carl Zeiss Meditec, Dublin, CA), the most commonly used time-domain OCT (TD-OCT) produces cross-sectional images with an axial resolution of 8 – 10μm and a transverse resolution of approximately 20μm. Peripapillary RNFL thickness measurements are obtained using a 3.4 mm diameter circular scan centered on the ONH. RNFL thickness is automatically determined and reported as an overall mean, by quadrants, and by clock hours. Quantitative information is also provided for the ONH structures and for total macular thickness.

TD-OCT RNFL and ONH measurements have been shown to discriminate well between healthy and glaucomatous eyes.[4; 7; 39; 40; 45; 67] Mean RNFL thickness, inferior quadrant and superior quadrant RNFL thickness provide the best diagnostic accuracy. There is good measurement reproducibility for both diffuse and focal RNFL defects.[3; 5; 6; 21; 47; 54]

Spectral-domain OCT (SD-OCT)—SD-OCT is a newer generation of the OCT technology offering several benefits over TD-OCT, such as enhanced resolution (3–6 μm axial resolution) and faster scanning (40–110 times faster with commercial SD-OCT systems).[51] Unlike TD-OCT, which requires the use of a moving reference mirror to record the depth information of the reflections from the target tissue, SD-OCT captures this information in the frequency domain, enabling all the reflections included in one A-scan to be captured simultaneously.[64] Moreover, SD-OCT offers image registration and 3D rendering capabilities. These advantages result in improved measurement reproducibility compared with TD-OCT.[18; 27; 33; 51] Although most studies showed that the glaucoma diagnostic ability of SD-OCT is similar to TD-OCT,[9; 33; 51; 55; 61] SD-OCT has an improved capability in early-stage glaucoma detection.[46] Figure 1 shows an example of an early glaucomatous damage detected by SD-OCT.

Scanning Laser Polarimetry

SLP (GDx, Carl Zeiss Meditec, Dublin, CA) determines the peripapillary RNFL thickness by measuring the amount of the retardation of polarized light, which is linearly correlated with the birefringent properties of the retina. As a result of the parallel orientation of the microtubules within the RGC axons, a change in the polarization of light, called retardation, occurs when light passes through the RNFL. This change can be quantified and is proportionate to the thickness of the RNFL.[63] The most recent commercially available iterations of this technology are named GDx VCC (Variable Corneal Compensator), GDx ECC (Enhanced Corneal Compensator), and GDx PRO. These devices provide individualized compensation for the birefringence of the media (mainly the cornea). The ECC version is an improvement over VCC resolving most of atypical retardation patterns (ARPs) that confound RNFL thickness measurement in a substantial subset of healthy and glaucomatous eyes. GDx provides reproducible measurement of RNFL thickness.[13; 23; 63; 69] GDx VCC outperforms the earlier iterations of this technology that used fixed corneal compensation in its ability to discriminate between healthy and glaucomatous eyes.[12; 20; 59; 62] GDx ECC performs better than VCC in the detection of early glaucoma.[36; 56] GDx NFI (Nerve Fiber Index), a machine classifier parameter that combines several measurements, consistently offers the best diagnostic performance.[14; 15; 50] However, this parameter is no longer available in most recent iterations of this technology and average TSNIT, quantifying the RNFL thickness, is the best diagnostic parameter among the existing parameters. Figure 2 shows an example of an early glaucomatous damage detected by the GDx PRO device.

Confocal Scanning Laser Ophthalmoscopy

The CSLO (Heidelberg Retina Tomograph (HRT); Heidelberg Engineering, Heidelberg, Germany) uses a 670nm diode laser beam with a confocal detector device that scans the ONH and provides three-dimensional measurements of ONH topography. It then generates a number of stereometric parameters, such as rim area, cup area, rim volume, and cup-to-disc ratio. The device has good reproducibility[10; 16; 30] and glaucoma discriminating ability,[2; 41; 44; 65; 66] comparable to optic disc assessment by glaucoma experts.[65] In Ocular Hypertension Treatment Study participants, HRT was able to detect structural glaucomatous changes up to eight years before functional defects were seen on VF testing.[71]

The latest version of the CLSO, the HRT III, offers a large normative database as well as advanced analytical tools such as the Moorfields Regression Analysis (MRA)[66] and the Glaucoma Probability Score (GPS).[58] The MRA improves the diagnostic accuracy of the instrument by using the global and sectoral neuroretinal rim area adjusted for disc size and age. This method is highly capable of discriminating between healthy and glaucomatous eyes.[42; 66] The GPS provides disease probability scores and minimizes operator error by relying on an automated approach to the optic disc classifying procedure. The discrimination ability of the GPS is similar to the MRA.[8] An example of early glaucomatous damage detected by the HRT III is shown in Figure 3.

Comparison of imaging technologies for glaucoma diagnosis

Studies comparing the glaucoma discriminating ability of TD-OCT, GDx and HRT[19; 40; 70] demonstrated that the best parameters of all three instruments performed similarly. Subjective evaluation of the ONH by glaucoma experts was as good as the objective imaging modalities in discriminating glaucomatous and healthy eyes; however, this may not reflect common clinical practice as it has been shown that glaucoma experts perform better than general ophthalmologists.[1] Indeed, it has been recently demonstrated that the diagnostic ability of the three imaging techniques was better than subjective assessment of the ONH by general ophthalmologists.[60]

SD-OCT may outperform SLP and CSLO in ability to diagnose glaucomatous damage. VF defects correlated better with RNFL thickness loss measured by SD-OCT compared to RNFL thinning as measured by SLP.[25] SD-OCT may have a higher sensitivity for glaucoma detection than HRT.[35]

Monitoring of glaucoma progression

Glaucomatous progression typically occurs either as a continuous linear process where tissue and function are gradually affected or in a stepwise pattern where sudden damage caused by an acute event is followed by a period of minimal change that lasts until another acute event takes place. In some individuals these two scenarios may coexist or they can occur in different phases of the disease. As the exact mode of progression in a given subject cannot be easily predicted, the assessment of glaucomatous progression requires clinical judgment as well as event- and trend-based analyses. In trend analysis, regression analysis of a dependent variable (e.g. RNFL thickness) on serial measurements provides progression rate over time. In event analysis, progression occurs when a follow-up measurement exceeds a pre-established threshold for change from baseline.

In clinical practice automated perimetry has been the standard for detecting glaucoma progression. In many subjects, however, structural damage precedes VF changes or occurs without simultaneous progressive VF changes.[43; 48; 57] This creates the need for tools capable of reliable and objective evaluation of progressive structural changes. Longitudinal assessment of glaucoma with imaging devices poses a significant challenge because of the rapidly evolving technology and resulting frequent software and hardware changes. Moreover, because of the lack of commonly acceptable reference standard that can be used to indicate progressive glaucomatous change, it is difficult to determine whether progression detected by an imaging device in the absence of VF loss reflects structural changes preceding functional loss as measured by SAP or is a false positive.

Most OCT progression studies use TD-OCT because of the longer follow up period.[68, 31; 32; 37] In a study on 64 glaucomatous and glaucoma suspect eyes followed for a mean period of 4.7 years, progression events defined by OCT occurred more frequently than progression events defined by VF.[68] The OCT progression studies in which progression was defined based on red-free fundus photographs demonstrated that analyzing both the mean and sectoral RNFL thicknesses is important in maximizing the detection of progression.[31; 32]

The inferotemporal (7 o'clock) sector and inferior quadrant RNFL thickness are most predictive of progression.[24; 28; 32; 37]

The advantages offered by SD-OCT result in improved intra-visit and inter-visit measurement reproducibility, indicating this instrument's potential for detecting early progression. In a recently published longitudinal study comparing SD-OCT with TDOCT, out of 128 glaucomatous eyes that were followed for a minimum of two years, 19 and 4 eyes were identified as progressing with SD-OCT and TD-OCT, respectively.[34] Figure 4 shows an example of glaucomatous progression detected by SD-OCT.

SLP derived structural measurements have a higher sensitivity for progression detection than SAP.[11] In a recent study evaluating progression with GDx-ECC, rates of RNFL loss were significantly greater in eyes that showed evidence of glaucoma progression based on SAP and/or optic disc stereophotographs compared to eyes that remained stable.[38] The GDx-ECC version of this technology performed significantly better than the VCC version for detection of change, suggesting that it could improve longitudinal evaluation of the RNFL. Figure 5 shows an example of glaucomatous progression detected by GDx.

Several longitudinal studies compare HRT with optic disc stereophotography and SAP in glaucomatous patients. In these studies, progression identified by HRT's topographic change analysis (TCA) was more frequent than progression identified with expert stereophotographic assessment of ONH and progression identified by SAP.[17; 29] There was a poor agreement, however, among the three techniques. The discrepancy was attributed to the inability of HRT change analysis to detect features such as splinter hemorrhages or defects in nerve fiber layer. HRT can detect small topographical changes that are otherwise not easily appreciated. Figure 6 shows an example of glaucomatous progression detected by HRT.

Conclusion

Imaging devices play an essential role in the diagnosis of glaucoma by providing a set of objective quantitative measurements and statistical classifications using comparisons to normative data. They cannot, however, reliably detect certain abnormal features such as an optic disc hemorrhage or disc pallor and therefore should not replace a clinical examination. Instead, they provide important complementary information intended to assist the clinician in the diagnostic process. As these technologies undergo constant evolution, their capabilities continue to improve, both for disease detection and identification of progression. None of the three main imaging modalities has been reliably demonstrated to be superior to another, although recently published studies using SD-OCT indicate that this technology may outperform SLP and CSLO in its ability to detect glaucomatous damage. Imaging-derived measures of progression have been shown to be more sensitive to change than SAP but, without the reference measure of progression, the reliability of these measures remains unknown. Due to the temporal dissociation between structure and function and the fact that glaucoma is a slowly progressive disease, longer follow-up periods are needed to establish whether structural changes identified with these imaging technologies can predict the subsequent development of VF loss. Because imaging may falsely identify glaucoma and its

progression, clinical management decisions should always be based on a combination of structural and functional measures and the results of a clinical examination.

Acknowledgments

Financial Support: Supported in part by National Institute of Health grants R01-EY13178, and P30-EY08098 (Bethesda, MD), The Eye and Ear Foundation (Pittsburgh, PA) and an unrestricted grant from Research to Prevent Blindness (New York, NY).

References

1. Abrams LS, Scott IU, Spaeth GL, et al. Agreement among optometrists, ophthalmologists, and residents in evaluating the optic disc for glaucoma. Ophthalmology. 1994; 101:1662–1667. [PubMed: 7936564]
2. Bathija R, Zangwill L, Berry CC, et al. Detection of early glaucomatous structural damage with confocal scanning laser tomography. J Glaucoma. 1998; 7:121–127. [PubMed: 9559499]
3. Blumenthal EZ, Williams JM, Weinreb RN, et al. Reproducibility of nerve fiber layer thickness measurements by use of optical coherence tomography. Ophthalmology. 2000; 107:2278–2282. [PubMed: 11097610]
4. Bowd C, Zangwill LM, Berry CC, et al. Detecting early glaucoma by assessment of retinal nerve fiber layer thickness and visual function. Invest Ophthalmol Vis Sci. 2001; 42:1993–2003. [PubMed: 11481263]
5. Budenz DL, Chang RT, Huang X, et al. Reproducibility of retinal nerve fiber thickness measurements using the stratus OCT in normal and glaucomatous eyes. Invest Ophthalmol Vis Sci. 2005; 46:2440–2443. [PubMed: 15980233]
6. Budenz DL, Fredette MJ, Feuer WJ, Anderson DR. Reproducibility of peripapillary retinal nerve fiber thickness measurements with stratus OCT in glaucomatous eyes. Ophthalmology. 2008; 115:661–666. e4. [PubMed: 17706287]
7. Budenz DL, Michael A, Chang RT, et al. Sensitivity and specificity of the StratusOCT for perimetric glaucoma. Ophthalmology. 2005; 112:3–9. [PubMed: 15629813]
8. Burgansky-Eliash Z, Wollstein G, Bilonick RA, et al. Glaucoma detection with the Heidelberg retina tomograph 3. Ophthalmology. 2007; 114:466–471. [PubMed: 17141321]
9. Chang RT, Knight OJ, Feuer WJ, Budenz DL. Sensitivity and specificity of timedomain versus spectral-domain optical coherence tomography in diagnosing early to moderate glaucoma. Ophthalmology. 2009; 116:2294–2299. [PubMed: 19800694]
10. Chauhan BC, LeBlanc RP, McCormick TA, Rogers JB. Test-retest variability of topographic measurements with confocal scanning laser tomography in patients with glaucoma and control subjects. Am J Ophthalmol. 1994; 118:9–15. [PubMed: 8023882]
11. Chauhan BC, McCormick TA, Nicolela MT, LeBlanc RP. Optic disc and visual field changes in a prospective longitudinal study of patients with glaucoma: comparison of scanning laser tomography with conventional perimetry and optic disc photography. Arch Ophthalmol. 2001; 119:1492–1499. [PubMed: 11594950]
12. Choplin NT, Zhou Q, Knighton RW. Effect of individualized compensation for anterior segment birefringence on retinal nerve fiber layer assessments as determined by scanning laser polarimetry. Ophthalmology. 2003; 110:719–725. [PubMed: 12689893]
13. Colen TP, Tjon-Fo-sang MJ, Mulder PG, Lemij HG. Reproducibility of measurements with the nerve fiber analyzer (NfA/GDx). J Glaucoma. 2000; 9:363–370. [PubMed: 11039737]
14. Da Pozzo S, Fuser M, Vattovani O, et al. GDx-VCC performance in discriminating normal from glaucomatous eyes with early visual field loss. Graefes Arch Clin Exp Ophthalmol. 2006; 244:689–695. [PubMed: 16292656]
15. Da Pozzo S, Iacono P, Marchesan R, et al. Scanning laser polarimetry with variable corneal compensation and detection of glaucomatous optic neuropathy. Graefes Arch Clin Exp Ophthalmol. 2005; 243:774–779. [PubMed: 15756574]

16. Dreher AW, Tso PC, Weinreb RN. Reproducibility of topographic measurements of the normal and glaucomatous optic nerve head with the laser tomographic scanner. Am J Ophthalmol. 1991; 111:221–229. [PubMed: 1992744]

17. Fayers T, Strouthidis NG, Garway-Heath DF. Monitoring glaucomatous progression using a novel Heidelberg Retina Tomograph event analysis. Ophthalmology. 2007; 114:1973–1980. [PubMed: 17662455]

18. Garas A, Vargha P, Hollo G. Reproducibility of retinal nerve fiber layer and macular thickness measurement with the RTVue-100 optical coherence tomograph. Ophthalmology. 2010; 117:738–746. [PubMed: 20079538]

19. Greaney MJ, Hoffman DC, Garway-Heath DF, et al. Comparison of optic nerve imaging methods to distinguish normal eyes from those with glaucoma. Invest Ophthalmol Vis Sci. 2002; 43:140–145. [PubMed: 11773024]

20. Greenfield DS, Knighton RW, Feuer WJ, et al. Correction for corneal polarization axis improves the discriminating power of scanning laser polarimetry. Am J Ophthalmol. 2002; 134:27–33. [PubMed: 12095804]

21. Gurses-Ozden R, Teng C, Vessani R, et al. Macular and retinal nerve fiber layer thickness measurement reproducibility using optical coherence tomography (OCT-3). J Glaucoma. 2004; 13:238–244. [PubMed: 15118470]

22. Harwerth RS, Carter-Dawson L, Shen F, et al. Ganglion cell losses underlying visual field defects from experimental glaucoma. Invest Ophthalmol Vis Sci. 1999; 40:2242–2250. [PubMed: 10476789]

23. Hoh ST, Ishikawa H, Greenfield DS, et al. Peripapillary nerve fiber layer thickness measurement reproducibility using scanning laser polarimetry. J Glaucoma. 1998; 7:12–15. [PubMed: 9493109]

24. Hollo G, Suveges I, Nagymihaly A, Vargha P. Scanning laser polarimetry of the retinal nerve fibre layer in primary open angle and capsular glaucoma. Br J Ophthalmol. 1997; 81:857–861. [PubMed: 9486026]

25. Horn FK, Mardin CY, Laemmer R, et al. Correlation between local glaucomatous visual field defects and loss of nerve fiber layer thickness measured with polarimetry and spectral domain OCT. Invest Ophthalmol Vis Sci. 2009; 50:1971–1977. [PubMed: 19151389]

26. Huang D, Swanson EA, Lin CP, et al. Optical coherence tomography. Science. 1991; 254:1178–1181. [PubMed: 1957169]

27. Kim JS, Ishikawa H, Sung KR, et al. Retinal nerve fibre layer thickness measurement reproducibility improved with spectral domain optical coherence tomography. Br J Ophthalmol. 2009; 93:1057–1063. [PubMed: 19429591]

28. Kook MS, Sung K, Park RH, et al. Reproducibility of scanning laser polarimetry (GDx) of peripapillary retinal nerve fiber layer thickness in normal subjects. Graefes Arch Clin Exp Ophthalmol. 2001; 239:118–121. [PubMed: 11372540]

29. Kourkoutas D, Buys YM, Flanagan JG, et al. Comparison of glaucoma progression evaluated with Heidelberg retina tomograph II versus optic nerve head stereophotographs. Can J Ophthalmol. 2007; 42:82–88. [PubMed: 17361246]

30. Kruse FE, Burk RO, Volcker HE, et al. Reproducibility of topographic measurements of the optic nerve head with laser tomographic scanning. Ophthalmology. 1989; 96:1320–1324. [PubMed: 2780001]

31. Lee EJ, Kim TW, Park KH, et al. Ability of Stratus OCT to detect progressive retinal nerve fiber layer atrophy in glaucoma. Invest Ophthalmol Vis Sci. 2009; 50:662–668. [PubMed: 18824734]

32. Leung CK, Cheung CY, Weinreb RN, et al. Evaluation of retinal nerve fiber layer progression in glaucoma: a study on optical coherence tomography guided progression analysis. Invest Ophthalmol Vis Sci. 2010; 51:217–222. [PubMed: 19684001]

33. Leung CK, Cheung CY, Weinreb RN, et al. Retinal nerve fiber layer imaging with spectral-domain optical coherence tomography: a variability and diagnostic performance study. Ophthalmology. 2009; 116:1257–1263. 63 e1-2. [PubMed: 19464061]

34. Leung CK, Chiu V, Weinreb RN, et al. Evaluation of Retinal Nerve Fiber Layer Progression in Glaucoma A Comparison between Spectral-Domain and Time-Domain Optical Coherence Tomography. Ophthalmology. 2011

35. Leung CK, Ye C, Weinreb RN, et al. Retinal nerve fiber layer imaging with spectraldomain optical coherence tomography a study on diagnostic agreement with Heidelberg Retinal Tomograph. Ophthalmology. 2010; 117:267–274. [PubMed: 19969364]
36. Medeiros FA, Bowd C, Zangwill LM, et al. Detection of glaucoma using scanning laser polarimetry with enhanced corneal compensation. Invest Ophthalmol Vis Sci. 2007; 48:3146–3153. [PubMed: 17591884]
37. Medeiros FA, Zangwill LM, Alencar LM, et al. Detection of glaucoma progression with stratus OCT retinal nerve fiber layer, optic nerve head, and macular thickness measurements. Invest Ophthalmol Vis Sci. 2009; 50:5741–5748. [PubMed: 19815731]
38. Medeiros FA, Zangwill LM, Alencar LM, et al. Rates of progressive retinal nerve fiber layer loss in glaucoma measured by scanning laser polarimetry. Am J Ophthalmol. 2010; 149:908–915. [PubMed: 20378095]
39. Medeiros FA, Zangwill LM, Bowd C, et al. Evaluation of retinal nerve fiber layer, optic nerve head, and macular thickness measurements for glaucoma detection using optical coherence tomography. Am J Ophthalmol. 2005; 139:44–55. [PubMed: 15652827]
40. Medeiros FA, Zangwill LM, Bowd C, Weinreb RN. Comparison of the GDx VCC scanning laser polarimeter, HRT II confocal scanning laser ophthalmoscope, and stratus OCT optical coherence tomograph for the detection of glaucoma. Arch Ophthalmol. 2004; 122:827–837. [PubMed: 15197057]
41. Miglior S, Casula M, Guareschi M, et al. Clinical ability of Heidelberg retinal tomograph examination to detect glaucomatous visual field changes. Ophthalmology. 2001; 108:1621–1627. [PubMed: 11535460]
42. Miglior S, Guareschi M, Albe E, et al. Detection of glaucomatous visual field changes using the Moorfields regression analysis of the Heidelberg retina tomograph. Am J Ophthalmol. 2003; 136:26–33. [PubMed: 12834666]
43. Miglior S, Zeyen T, Pfeiffer N, et al. Results of the European Glaucoma Prevention Study. Ophthalmology. 2005; 112:366–375. [PubMed: 15745761]
44. Mikelberg FS, Parfitt CM, Swindale NV, et al. Ability of the heidelberg retina tomograph to detect early glaucomatous visual field loss. J Glaucoma. 1995; 4:242–247. [PubMed: 19920681]
45. Nouri-Mahdavi K, Hoffman D, Tannenbaum DP, et al. Identifying early glaucoma with optical coherence tomography. Am J Ophthalmol. 2004; 137:228–235. [PubMed: 14962410]
46. Park SB, Sung KR, Kang SY, et al. Comparison of glaucoma diagnostic Capabilities of Cirrus HD and Stratus optical coherence tomography. Arch Ophthalmol. 2009; 127:1603–1609. [PubMed: 20008715]
47. Paunescu LA, Schuman JS, Price LL, et al. Reproducibility of nerve fiber thickness, macular thickness, and optic nerve head measurements using StratusOCT. Invest Ophthalmol Vis Sci. 2004; 45:1716–1724. [PubMed: 15161831]
48. Quigley HA, Katz J, Derick RJ, et al. An evaluation of optic disc and nerve fiber layer examinations in monitoring progression of early glaucoma damage. Ophthalmology. 1992; 99:19–28. [PubMed: 1741133]
49. Quigley HA, Miller NR, George T. Clinical evaluation of nerve fiber layer atrophy as an indicator of glaucomatous optic nerve damage. Arch Ophthalmol. 1980; 98:1564–1571. [PubMed: 7425916]
50. Reus NJ, Lemij HG. Diagnostic accuracy of the GDx VCC for glaucoma. Ophthalmology. 2004; 111:1860–1865. [PubMed: 15465547]
51. Schuman JS. Spectral domain optical coherence tomography for glaucoma (an AOS thesis). Trans Am Ophthalmol Soc. 2008; 106:426–458. [PubMed: 19277249]
52. Schuman JS, Hee MR, Arya AV, et al. Optical coherence tomography: a new tool for glaucoma diagnosis. Curr Opin Ophthalmol. 1995; 6:89–95. [PubMed: 10150863]
53. Schuman JS, Hee MR, Puliafito CA, et al. Quantification of nerve fiber layer thickness in normal and glaucomatous eyes using optical coherence tomography. Arch Ophthalmol. 1995; 113:586–596. [PubMed: 7748128]
54. Schuman JS, Pedut-Kloizman T, Hertzmark E, et al. Reproducibility of nerve fiber layer thickness measurements using optical coherence tomography. Ophthalmology. 1996; 103:1889–1898. [PubMed: 8942887]

55. Sehi M, Grewal DS, Sheets CW, Greenfield DS. Diagnostic ability of Fourier-domain vs time-domain optical coherence tomography for glaucoma detection. Am J Ophthalmol. 2009; 148:597–605. [PubMed: 19589493]
56. Sehi M, Guaqueta DC, Feuer WJ, Greenfield DS. Scanning laser polarimetry with variable and enhanced corneal compensation in normal and glaucomatous eyes. Am J Ophthalmol. 2007; 143:272–279. [PubMed: 17157800]
57. Sommer A, Katz J, Quigley HA, et al. Clinically detectable nerve fiber atrophy precedes the onset of glaucomatous field loss. Arch Ophthalmol. 1991; 109:77–83. [PubMed: 1987954]
58. Swindale NV, Stjepanovic G, Chin A, Mikelberg FS. Automated analysis of normal and glaucomatous optic nerve head topography images. Invest Ophthalmol Vis Sci. 2000; 41:1730–1742. [PubMed: 10845593]
59. Tannenbaum DP, Hoffman D, Lemij HG, et al. Variable corneal compensation improves discrimination between normal and glaucomatous eyes with the scanning laser polarimeter. Ophthalmology. 2004; 111:259–264. [PubMed: 15019373]
60. Vessani RM, Moritz R, Batis L, et al. Comparison of quantitative imaging devices and subjective optic nerve head assessment by general ophthalmologists to differentiate normal from glaucomatous eyes. J Glaucoma. 2009; 18:253–261. [PubMed: 19295383]
61. Vizzeri G, Balasubramanian M, Bowd C, et al. Spectral domain-optical coherence tomography to detect localized retinal nerve fiber layer defects in glaucomatous eyes. Opt Express. 2009; 17:4004–4018. [PubMed: 19259242]
62. Weinreb RN, Bowd C, Zangwill LM. Glaucoma detection using scanning laser polarimetry with variable corneal polarization compensation. Arch Ophthalmol. 2003; 121:218–224. [PubMed: 12583788]
63. Weinreb RN, Shakiba S, Zangwill L. Scanning laser polarimetry to measure the nerve fiber layer of normal and glaucomatous eyes. Am J Ophthalmol. 1995; 119:627–636. [PubMed: 7733188]
64. Wojtkowski M, Leitgeb R, Kowalczyk A, et al. In vivo human retinal imaging by Fourier domain optical coherence tomography. J Biomed Opt. 2002; 7:457–463. [PubMed: 12175297]
65. Wollstein G, Garway-Heath DF, Fontana L, Hitchings RA. Identifying early glaucomatous changes. Comparison between expert clinical assessment of optic disc photographs and confocal scanning ophthalmoscopy. Ophthalmology. 2000; 107:2272–2277. [PubMed: 11097609]
66. Wollstein G, Garway-Heath DF, Hitchings RA. Identification of early glaucoma cases with the scanning laser ophthalmoscope. Ophthalmology. 1998; 105:1557–1563. [PubMed: 9709774]
67. Wollstein G, Ishikawa H, Wang J, et al. Comparison of three optical coherence tomography scanning areas for detection of glaucomatous damage. Am J Ophthalmol. 2005; 139:39–43. [PubMed: 15652826]
68. Wollstein G, Schuman JS, Price LL, et al. Optical coherence tomography longitudinal evaluation of retinal nerve fiber layer thickness in glaucoma. Arch Ophthalmol. 2005; 123:464–470. [PubMed: 15824218]
69. Zangwill L, Berry CA, Garden VS, Weinreb RN. Reproducibility of retardation measurements with the nerve fiber analyzer II. J Glaucoma. 1997; 6:384–389. [PubMed: 9407367]
70. Zangwill LM, Bowd C, Berry CC, et al. Discriminating between normal and glaucomatous eyes using the Heidelberg Retina Tomograph, GDx Nerve Fiber Analyzer, and Optical Coherence Tomograph. Arch Ophthalmol. 2001; 119:985–993. [PubMed: 11448320]
71. Zangwill LM, Weinreb RN, Beiser JA, et al. Baseline topographic optic disc measurements are associated with the development of primary open-angle glaucoma: the Confocal Scanning Laser Ophthalmoscopy Ancillary Study to the Ocular Hypertension Treatment Study. Arch Ophthalmol. 2005; 123:1188–1197. [PubMed: 16157798]

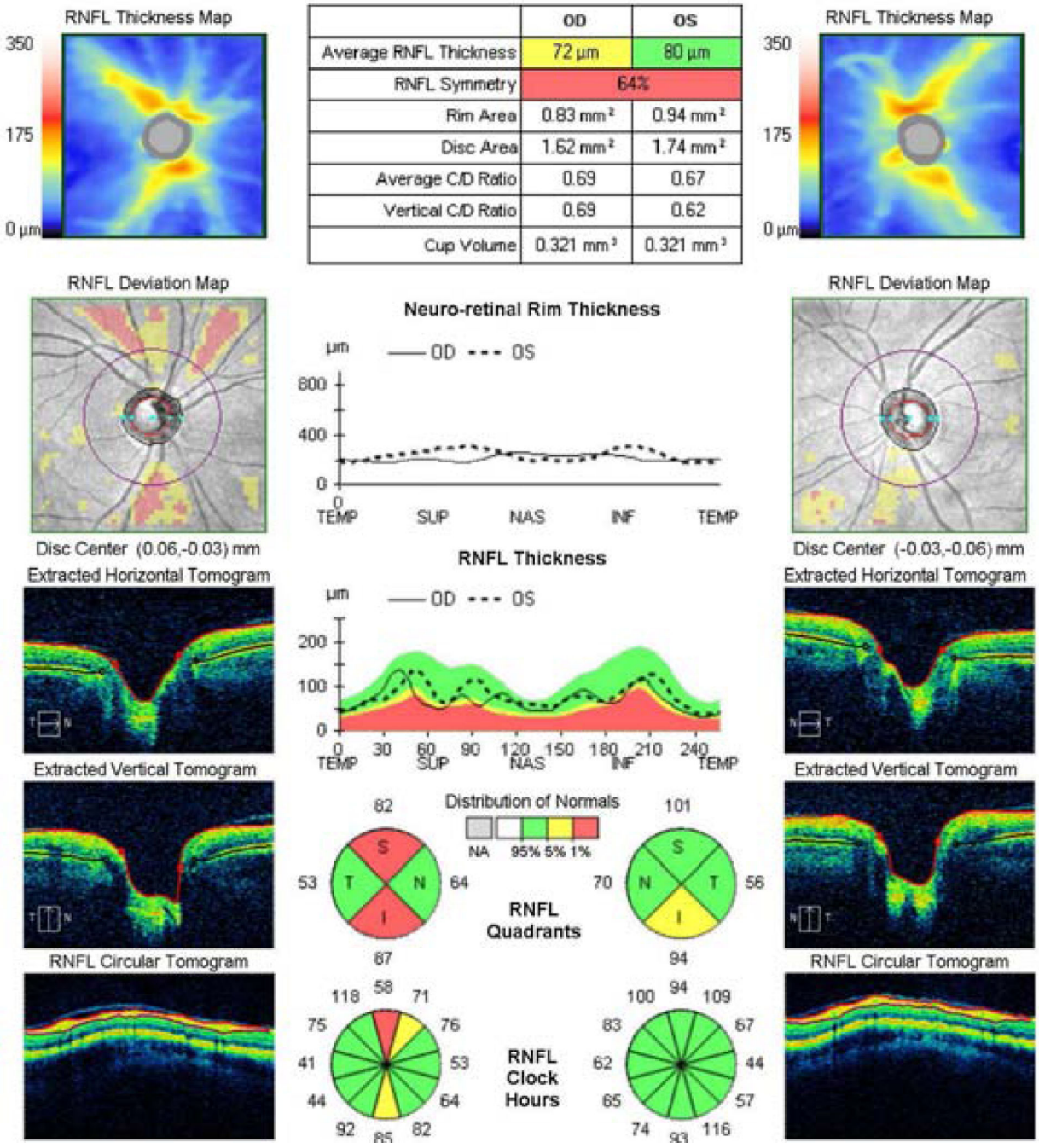

Figure 1.

Early glaucomatous damage as detected by spectral-domain optical coherence tomography. Wedge shaped thinning of the retinal nerve fiber layer (RNFL; red zones in the RNFL Deviation Map) are evident in the superior and inferior regions in the right eye. RNFL Thickness profile also demonstrates localized thinning in the same regions. Quantitative analysis shows deviation from normal range in the overall, quadrant and clock-hour RNFL thickness analysis.

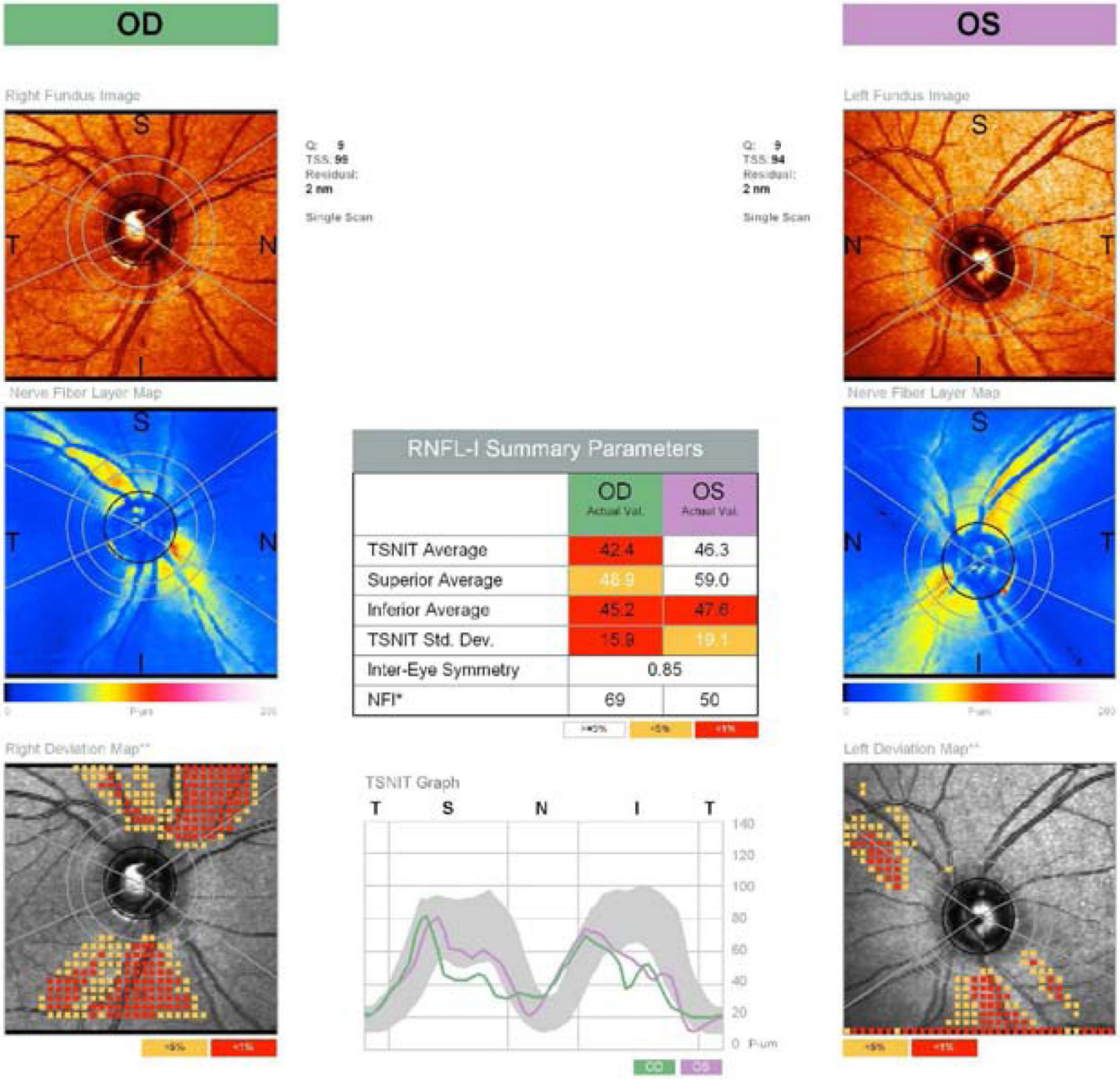

Figure 2.

Scanning laser polarimetry imaging showing superior and inferior retinal nerve fiber layer (RNFL) atrophy in the right eye and inferior RNFL atrophy in the left eye (deviation map). Compared with age matched healthy controls, several retardation parameters are outside normal limits and marked by the red background (RNFL Summary Parameters table).

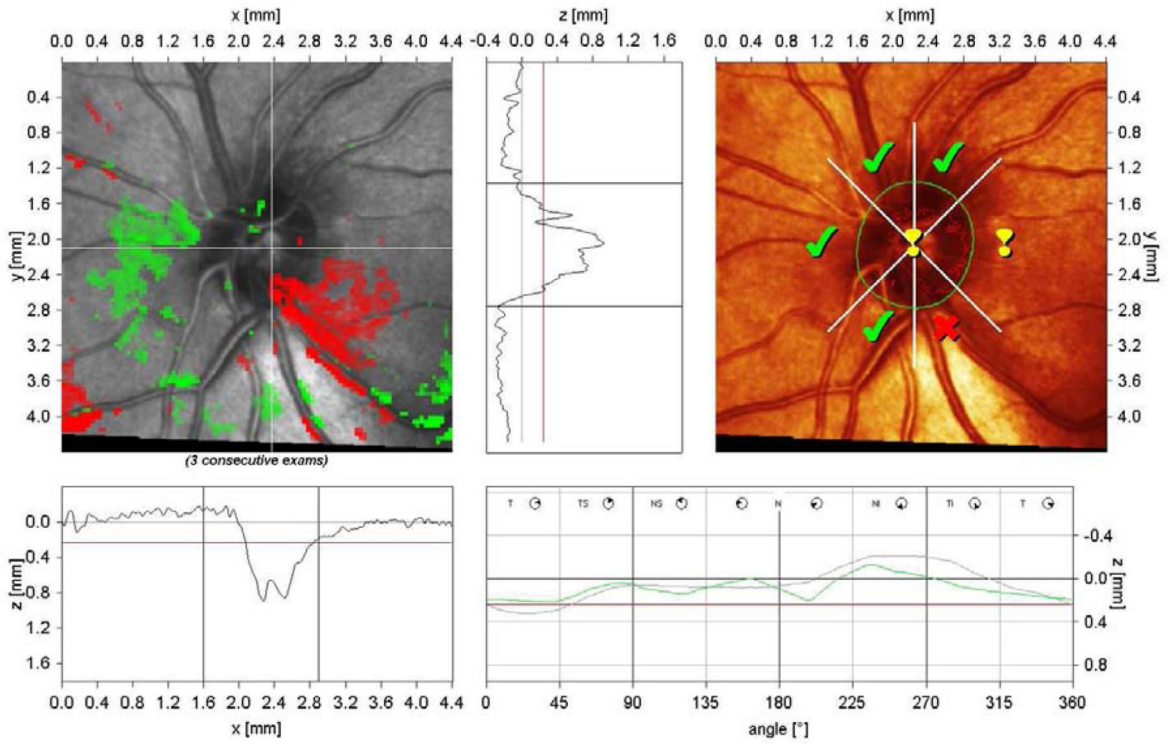

Stereometric Analysis ONH		Change	Normal
Disc Area	1.50	0.00 mm²	1.63 - 2.43
Cup Area	0.53	0.09 mm²	0.11 - 0.68
Rim Area	0.96	-0.09 mm²	1.31 - 1.96
Cup Volume	0.14	0.03 mm³	-0.01 - 0.18
Rim Volume	0.24	-0.02 mm³	0.30 - 0.61
Cup/Disc Area Ratio	0.36	0.06	0.07 - 0.30
Linear Cup/Disc Ratio	0.60	0.06	0.27 - 0.55
Mean Cup Depth	0.29	0.02 mm	0.10 - 0.27
Maximum Cup Depth	0.79	0.05 mm	0.32 - 0.76
Cup Shape Measure	-0.16	-0.02	-0.28 - -0.15
Height Variation Contour	0.35	-0.19 mm	0.31 - 0.49
Mean RNFL Thickness	0.15	-0.06 mm	0.20 - 0.32
RNFL Cross Sectional Area	0.64	-0.25 mm²	0.99 - 1.66
Reference Height	236	-22 µm	
Topography Std Dev.	28 µm		
FSM	-0.08		
RB	0.61		

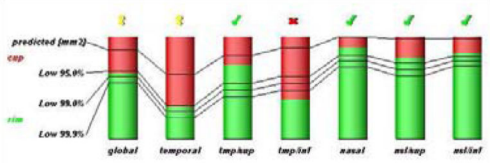

Moorfields Classification: Outside normal limits (*)

(*) Moorfields regression classification (Ophthalmology 1998;105:1557-1563). Classification based on statistics. Diagnosis is physician's responsibility.

Comments:

Date: Signature:

Figure 3.

Early glaucomatous damage as detected by Confocal Scanning Laser Ophthalmoscopy. Neuroretinal rim defect is marked in the temporal inferior region corresponding to an adjacent retinal nerve fiber layer defect (upper right). This region experienced a statistically significant deterioration from baseline as marked by the red region (upper left). Compared with healthy control data, several quantified parameters were outside the normal range.

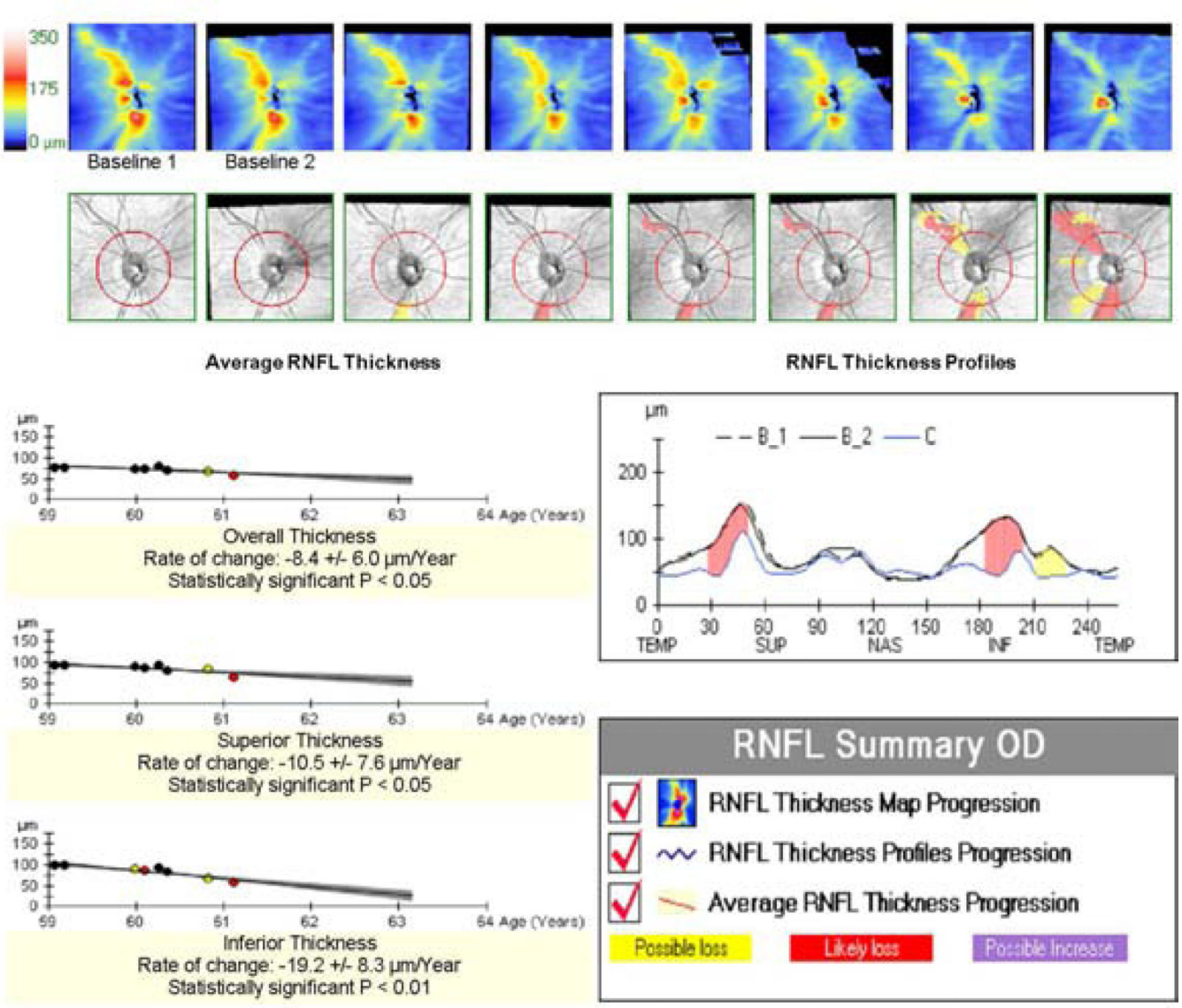

Figure 4.

Spectral-domain optical coherence tomography retinal nerve fiber layer (RNFL) Guided Progression Analysis. Likely progression (marked in red) is identified in the inferotemporal and superotemporal regions on the RNFL Thickness Map and RNFL Thickness Profiles Progression. Average RNFL Thickness Progression shows likely progression in the overall, inferior and superior sector thickness. Trend lines are drawn and rates of change are provided all of which show statistically significant rate of RNFL thinning.

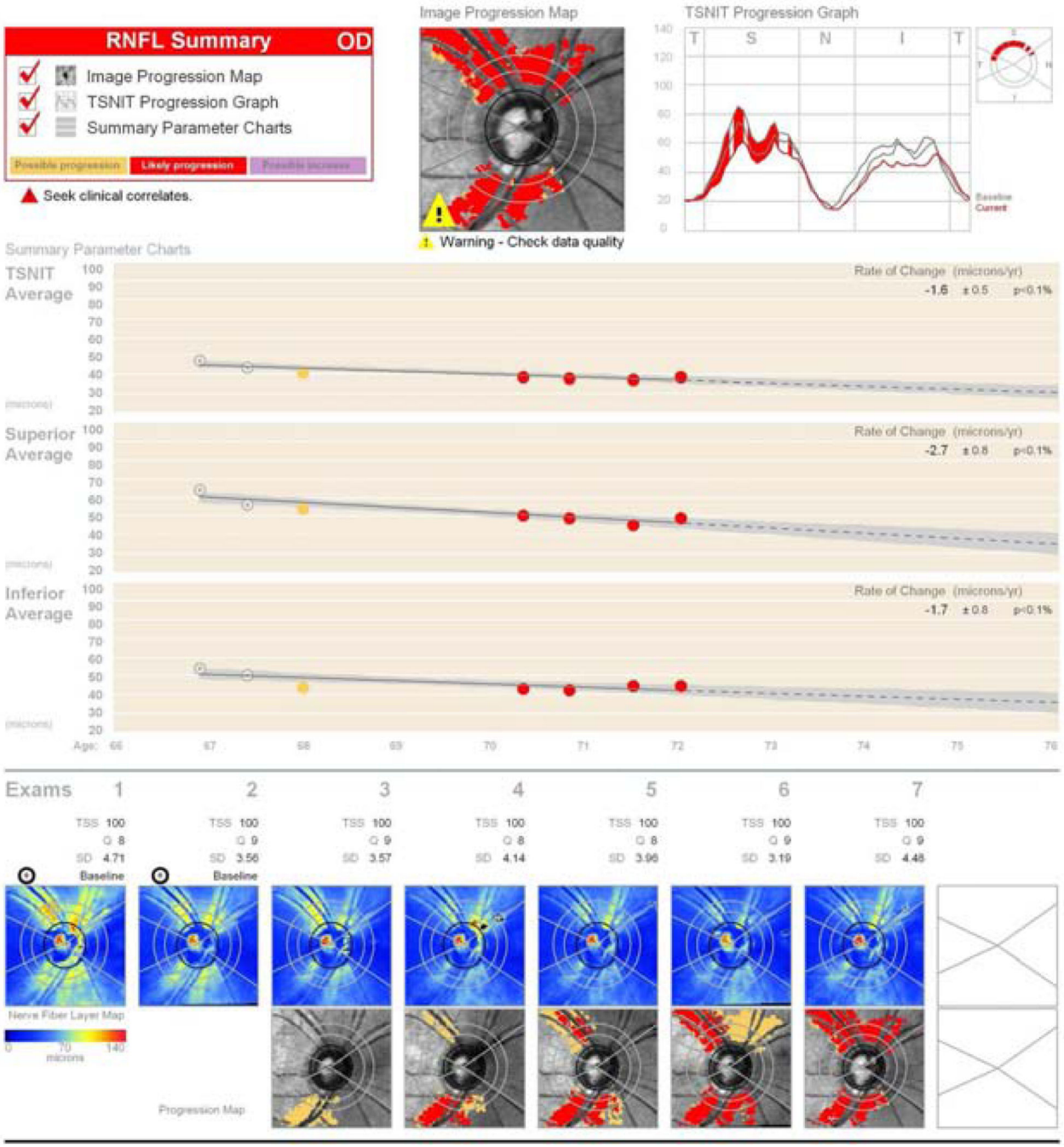

Figure 5.

Scanning laser polarimetry Guided Progression Analysis. The Image Progression Map shows progression in the inferotemporal and superotemporal regions. TSNIT Progression Graph shows progression in the superior region. Summary Parameter Charts show a significant decrease in TSNIT average, superior and inferior RNFL thicknesses.

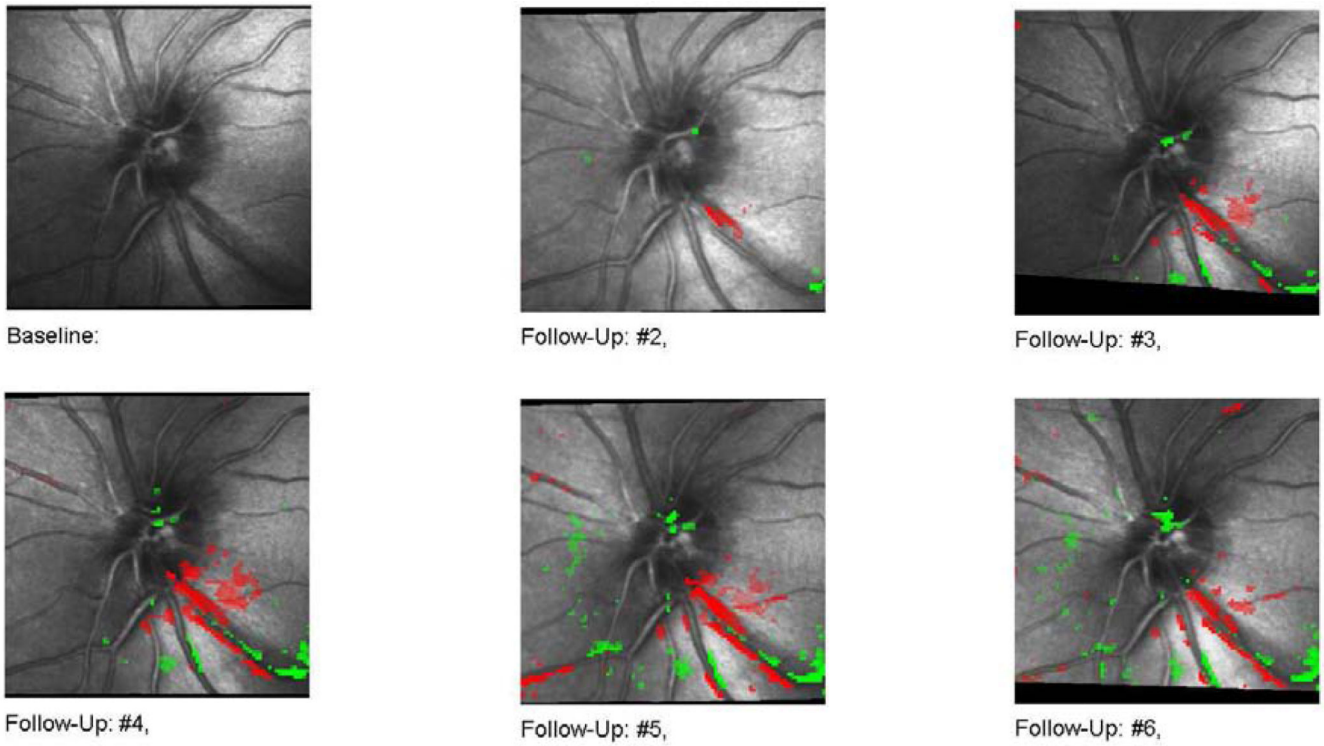

Figure 6.

Scanning laser ophthamoscopy Topographical Change Analysis (TCA). A surface height depression (red pixels on follow-up scans) can be seen initially in the inferotemporal region. Progressive wedge shaped enlargement of the depressed area is seen on the follow-up images.